Supporting information

Revisiting the Catalytic Role of Supported Na_2WO_4 for Oxidative Coupling of Methane Reaction

Zejing Wei [a†], Kunkun Wei [a†], Xutao Chen [a,*], Yang Pan [b], Chengyuan Liu[b], Liping Xiao [a], Yifeng Shi [a,*], Shihui Zou [c,*], Jie Fan [a,*]

[a]Zhejiang Key Laboratory of Low-Carbon Synthesis of Value-Added Chemicals, Zhejiang University, Hangzhou 310027, Zhejiang, China

[b]National Synchrotron Radiation Laboratory, University of Science and Technology of China, Hefei 230029, Anhui, China

[c]College of Materials Science and Engineering, Zhejiang University of Technology, Hangzhou 310014, Zhejiang, China

[†]These authors contributed equally to this work.

Table S1 Ionization threshold, adopted photo energy and m/z ratio of species. CO and CO_2 were acquired over a range of photon energies (14.61–14.79 eV) and averaged to improve measurement accuracy.

Species	**Ionization energy/eV**	**Photon energy/eV**	**m/z**
$\cdot CH_3$	9.84	11.00	15.02
CH_4	12.61	/	16.04
C_2H_4	10.47	11.00	28.00
C_2H_6	10.84	12.00	30.01
CO	14.01	14.61-14.79	27.96
CO_2	13.78	14.61-14.79	43.95

Table S2. Feeding and actual loading of Na_2WO_4 of the catalysts.

Na_2WO_4 feeding (wt.%)	**ICP-OES result (wt.%)**	
	Na_2WO_4/SiO_2	**Na_2WO_4/ZrO_2**
5	5.2	5.6
10	10.5	10.3
20	20.0	19.9
30	30.0	29.7
50	54.7	49.2
30-washed	13.4	3.7

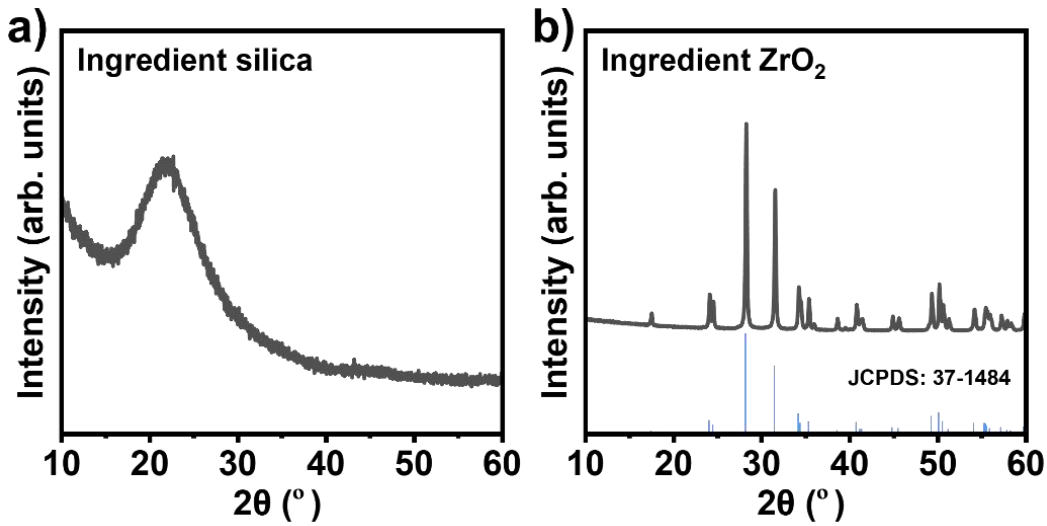


Figure S1. WAXRD pattern of ingredient silica and ZrO_2 used for synthesis.

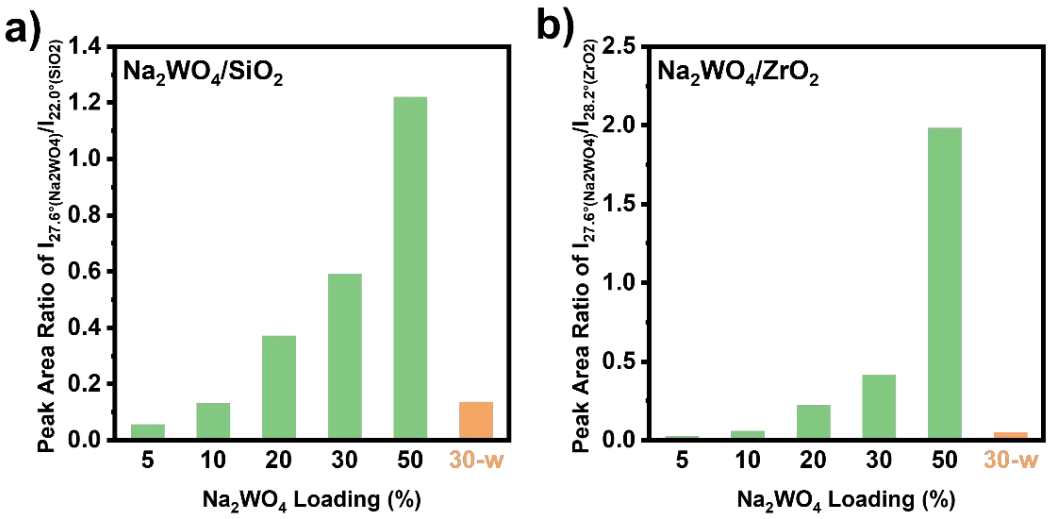


Figure S2. Ratio of the XRD peak areas of the strongest peak of Na_2WO_4 (2θ=27.6°) to the support (2θ=22.0° for SiO_2 and 2θ=28.5° for ZrO_2). a) Na_2WO_4/SiO_2, b) Na_2WO_4/ZrO_2.

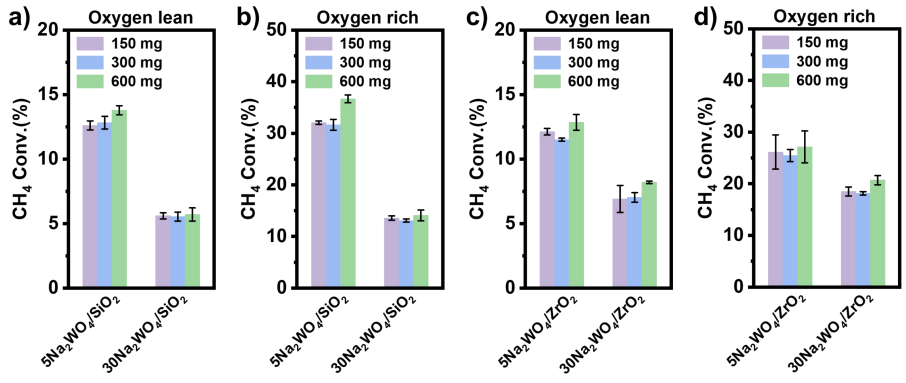


Figure S3. Effect of catalyst mass on OCM performance at a constant GHSV of 13400 mL $g_{catalyst}^{-1}$ h^{-1} under (a, c) oxygen-lean condition (CH_4:O_2:N_2=30:10:27) and (b, d) oxygen-rich condition (CH_4:O_2:N_2=30:10:27). Reaction temperature: (a, b) 800 °C and (c, d) 850 °C. The CH_4 conversion remains essentially constant across the entire evaluated mass range for different Na_2WO_4 loadings (5 and 30 wt.%), support materials (SiO_2 and ZrO_2), and feed gas compositions (oxygen-lean and oxygen-rich environments), confirming the absence of external mass transfer. In addition, the independence of CH_4 conversion from the catalyst particle size excludes internal diffusion limitations.

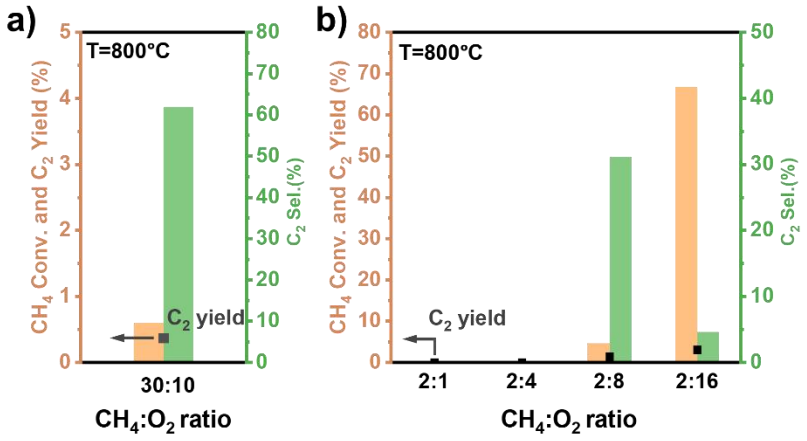


Figure S4. Catalytic performance of blank tube experiments under varying feed gas compositions. Total gas flow was fixed at 67 mL min^{-1} using N_2 as the balance gas. a) CH_4 flow rate was 30 mL min^{-1}; b) CH_4 flow rate was fixed at 2 mL min^{-1}.

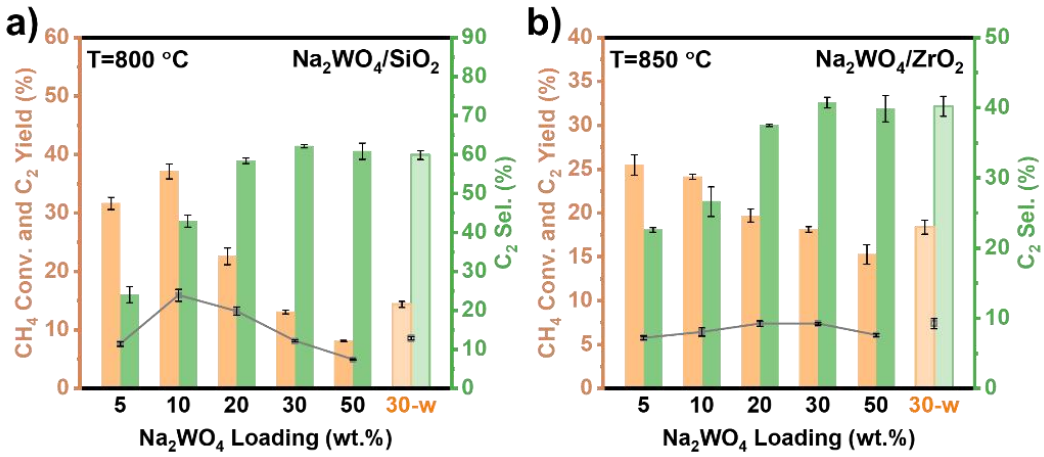


Figure S5. OCM performances of a) Na_2WO_4/SiO_2 and b) Na_2WO_4/ZrO_2 catalysts under oxygen-rich atmosphere. Reaction conditions: 300 mg catalyst, total gas flow rate 67 mL min^{-1}, CH_4:O_2:N_2=2:8:57.

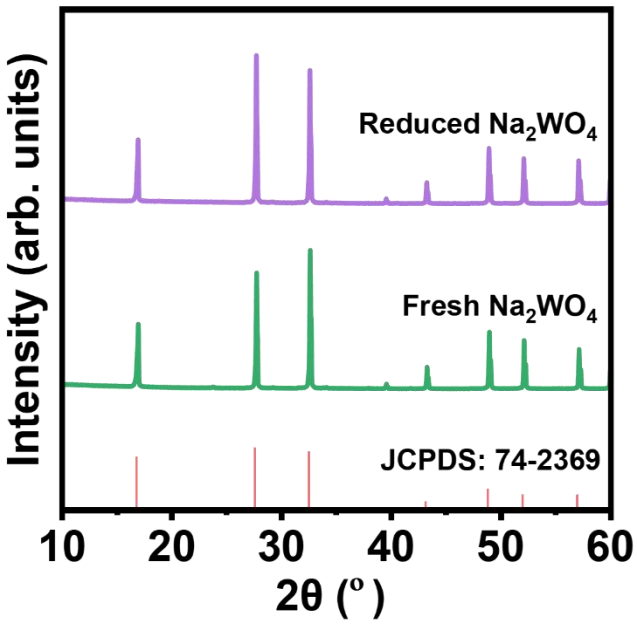


Figure S6. XRD of fresh and reduced Na_2WO_4. The reduced Na_2WO_4 was obtained by calcining fresh Na_2WO_4 at 850 °C for 5 hours under 10% H_2/Ar (flow rate 30 mL min^{-1}).

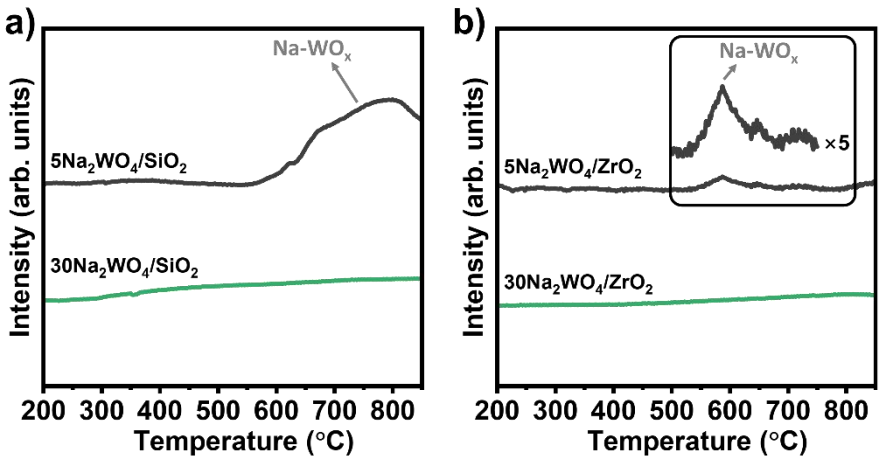


Figure S7. H_2-TPR profiles of (a) $5Na_2WO_4/SiO_2$ and $30Na_2WO_4/SiO_2$ and (b) $5Na_2WO_4/ZrO_2$ and $5Na_2WO_4/ZrO_2$ catalysts. To ensure the reliability of the results, we have repeated the H_2-TPR experiments using a 10% H_2/Ar mixture (30 mL min^{-1}) for four representative catalysts: $5Na_2WO_4/SiO_2$, $30Na_2WO_4/SiO_2$, $5Na_2WO_4/ZrO_2$, and $30Na_2WO_4/ZrO_2$. The results exhibit identical reduction behaviors and trends to those obtained under 10% H_2/He atmosphere (**Figure 5**), thereby fully corroborating our interpretations regarding the catalyst reducibility.

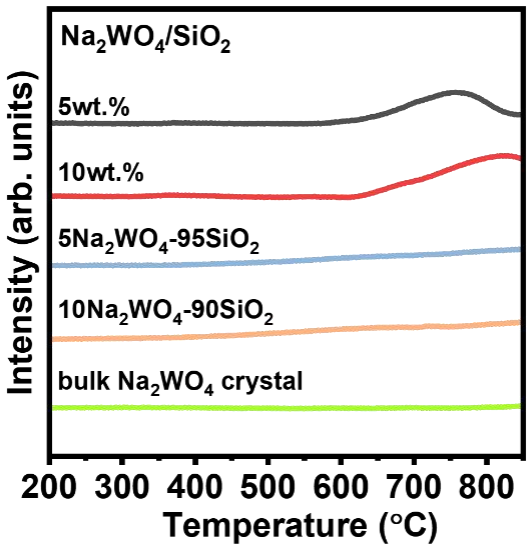


Figure S8. H_2-TPR profiles of $5Na_2WO_4/SiO_2$, $10Na_2WO_4/SiO_2$, $5Na_2WO_4$-$95SiO_2$, $10Na_2WO_4$-$90SiO_2$, and bulk Na_2WO_4 crystal. The reduction was performed using 50 mg of catalyst under a 10% H_2/He flow (30 mL min^{-1}) with a heating rate of 10 °C min^{-1}.

Table S3 Detailed data for in situ synchrotron-based VUV photoionization mass spectrometry studies. $[\bullet CH_3]_Q$, $[\bullet CH_3]_C$, $I(C_2H_4)$, $I(C_2H_6)$, I(CO), $I(CO_2)$ denoted the signal intensities of the corresponding species. $[\bullet CH_3]_Q$, $[\bullet CH_3]_C$, $I(C_2H_4)$ were obtained at the photo energy of 11 eV and $I(C_2H_6)$ of 12 eV. I(CO) and $I(CO_2)$ were acquired over a range of photon energies (14.61–14.79 eV, in 0.2 eV steps) and averaged to improve measurement accuracy.

Catalyst	T (°C)	$[\bullet CH_3]_Q$	$[\bullet CH_3]_C$	RE(%)	$I(C_2H_4)$	$I(C_2H_6)$	I(CO)	$I(CO_2)$
$5Na_2WO_4/SiO_2$	700	0.39	0.25	35.5	17.6	44.8	2.0	4.4
	750	0.52	0.21	59.2	29.0	43.2	1.9	4.4
	800	0.61	0.26	57.5	25.2	25.2	1.9	4.5
$30Na_2WO_4/SiO_2$	700	0.39	0.21	45.3	9.6	54.5	1.1	1.1
	750	0.52	0.17	67.6	43.1	81.8	1.6	2.3
	800	0.61	0.20	66.9	44.2	74.6	1.8	3.2
$30Na_2WO_4/SiO_2$-w	700	0.39	0.19	51.4	15.0	48.2	1.0	1.2
	750	0.52	0.18	66.3	29.0	63.7	1.3	1.9
	800	0.61	0.19	68.5	38.8	72.7	1.6	3.1
$5Na_2WO_4/ZrO_2$	700	0.39	0.33	16.1	8.9	25.2	1.0	1.4
	750	0.52	0.35	33.3	13.0	31.1	1.4	2.4
	800	0.61	0.41	33.1	13.6	30.9	1.6	2.7
$30Na_2WO_4/ZrO_2$	700	0.39	0.21	47.1	35.6	82.5	0.3	0.2
	750	0.52	0.26	50.3	48.0	86.0	0.5	0.4
	800	0.61	0.27	55.1	49.4	84.6	0.5	0.4
$30Na_2WO_4/ZrO_2$-w	700	0.39	0.23	41.4	20.5	76.0	0.2	0.2
	750	0.52	0.26	49.3	33.9	87.0	0.5	0.5
	800	0.61	0.25	59.7	31.4	80.0	0.8	0.9